



TITLE:

Response prediction of long flexible risers subject to forced harmonic vibration

AUTHOR(S):

Riveros, Carlos Alberto; Utsunomiya, Tomoaki;
Maeda, Katsuya; Itoh, Kazuaki

CITATION:

Riveros, Carlos Alberto ...[et al]. Response prediction of long flexible risers subject to forced harmonic vibration. *Journal of Marine Science and Technology* 2010, 15(1): 44-53

ISSUE DATE:

2010-03

URL:

<http://hdl.handle.net/2433/128770>

RIGHT:

The original publication is available at www.springerlink.com; この論文は出版社版ではありません。引用の際には出版社版をご確認ご利用ください。 ; This is not the published version. Please cite only the published version.

Response Prediction of Long Flexible Risers Subject to Forced Harmonic Vibration

C.A. Riveros¹, T. Utsunomiya², K. Maeda³ and K. Itoh⁴

¹Dr. Eng., Department of Civil and Earth Resources Engineering, Kyoto University,
(Katsura Campus, Nishikyo-ku, Kyoto 615-8540, Japan)

E-mail: riveros@udea.edu.co

²Dr. Eng., Department of Civil and Earth Resources Engineering, Kyoto University,
(Katsura Campus, Nishikyo-ku, Kyoto 615-8540, Japan)

E-mail: utsunomi@mbbox.kudpc.kyoto-u.ac.jp (Corresponding Author)

³Ph.D, Deep Sea Technology Research Group, National Maritime Research Institute,
(6-38-1, Shinkawa, Mitaka-shi, Tokyo 181-0004, Japan)

E-mail: kmaeda@nmri.go.jp

⁴Dr. Eng., Marine Technology and Development Program, Marine Technology Center,
JAMSTEC

(2-15, Natushima-cho, Yokosuka 237-0061, Japan)

E-mail: itohk@jamstec.go.jp

Abstract – Several research efforts have been directed toward the development of models for response prediction of flexible risers. The main difficulties arise from the fact that the dynamic response of flexible risers involves a highly nonlinear behavior and a self-regulated process. This paper presents a quasi-steady approach for response prediction of oscillating flexible risers. Amplitude-dependent lift coefficients and an increased mean drag coefficient model during synchronization events are considered. Experimental validation of the proposed model is carried out using a 20-meter riser model excited by forced harmonic vibration at its top end. Large variations in the hydrodynamic force coefficients, a low mass-ratio value and synchronization events are the main features of the model presented in this paper. Experimental validation is provided for the asymmetric, transverse, diagonal and third vortex regimes.

Keywords: flexible riser, vortex-induced vibration, beta parameter, synchronization event, mass-damping parameter.

1. Introduction

A great deal of attention has been given in recent years to meet the industry demands of providing riser systems for profitable oil extraction at water depths of 1000 m or more. In addition, there is an ongoing interest in the use of riser systems for carbon dioxide injection in deep sea. As a result, the research community is actively working on developing response prediction models for risers in order to comply with the aforementioned demands. However, the self-regulated nature of the Vortex-Induced Vibration (VIV) process, caused by vortices shed from a riser, is highly nonlinear and therefore its accurate prediction is still not possible. There are basically two approaches for predicting the dynamic response of a flexible riser. The main difference between these two approaches is related to the procedure employed to calculate hydrodynamic forces.

A Computational Fluid Dynamics (CFD)-based procedure to solve the Navier-Stokes equations is employed for the first approach in order to compute two-dimensional flow around the riser for each of the horizontal planes in which the riser is divided along its length. According to Sarpkaya¹, there currently exist several issues to be understood related to the complex nature of the coupling mechanism between the dynamics of the near-wake and that of the riser. Basically, Direct Numerical Simulation (DNS) and Large Eddy Simulation (LES) are capable of providing better representation of the wake-boundary-layer mechanism as compared to two-dimensional unsteady Reynolds-Averaged Navier-Stokes (RANS) simulations (Sarpkaya¹). However, as noted by Al-Jamal and Dalton², either 2-D or 3-D LES simulation is not capable of calculating the full flow past stationary cylinder, much less an oscillating one. On the other hand, DNS simulations are computationally demanding and therefore cannot be used in practical applications. Finally, turbulence remains poorly understood making CFD-based approach restricted for industrial design as reported by Sarpkaya¹.

The second approach is referred to as semi-empirical. In this approach, a flexible riser is usually modeled as a beam with low flexural stiffness making use of hydrodynamic force coefficients derived from experiments to calculate the hydrodynamic forces acting on the riser. Therefore, accurate response prediction is strongly related to the availability of reliable experimental data for the modeling conditions involved in a simulation. Chaplin et al.³ presented a comprehensive study on response prediction of

risers using experimental data obtained from a riser model excited in stepped current and blind predictions from 11 different response prediction models. Chaplin et al.³ showed that the semi-empirical approach is more successful at predicting the cross-flow response of a flexible riser than the CFD-based approach.

The quasi-steady assumption states that the dynamic response of an oscillating flexible riser can be approximated by using hydrodynamic force coefficients derived from experiments performed in fixed cylinders. Therefore, it is commonly accepted the use of force coefficients experimentally derived from oscillatory flow acting on a fixed cylinder to obtain the dynamic response of oscillating flexible risers. Furthermore, Obasaju et al.⁴ stated that “even though many different vortex patterns are exhibited in oscillatory flow, the basic mechanism that governs the rate at which vortices develop may be the same as in steady flow”.

This paper presents a response prediction model for oscillating flexible risers. It is based on the Finite Element Method (FEM) and the quasi-steady approach for the prediction of the cross-flow forces. A 20-meter riser model having a mass-ratio of 1.7 is used to experimentally validate the proposed model. Measurements were obtained at Keulegan-Carpenter (KC) numbers located in the asymmetric, transverse, diagonal and third vortex regimes (Obasaju et al.⁴). Therefore, it is provided a wide range of experimental validation. Amplitude-dependent lift coefficients and an increased mean drag model during synchronization of the shedding and oscillating frequencies are also included in the proposed model.

2. Response Prediction Model

The Euler-Bernoulli beam equation is used herein to model a riser idealized as a beam with low flexural stiffness following the procedure proposed by Huera-Huarte et al.⁵ as shown in Eq. (1). A Cartesian reference is defined in the x -axis by the direction of the flow velocity in the case of a stationary body or the in-line motion in the case of an oscillating body, the z -axis is defined in the direction of the riser's axis and the y -axis is perpendicular to both as shown in Fig.1.

$$EI \frac{\partial^4 u_{x,y}(z,t)}{\partial z^4} - \frac{\partial}{\partial z} \left[(T_t - w(L - |z|)) \frac{\partial u_{x,y}(z,t)}{\partial z} \right] + c_0 \frac{\partial u_{x,y}(z,t)}{\partial t} + m_0 \frac{\partial^2 u_{x,y}(z,t)}{\partial t^2} = F_{T_{x,y}}(z,t) \quad (1)$$

where m_0 is the mass of the riser per unit length, $u_{x,y}(z,t)$ is the deflection, c_0 is the damping coefficient, EI is the flexural stiffness, T_t is the tension applied at the top of the riser, L is the length of the riser and w is the submerged weight. The external fluid force is $F_{T_{x,y}}$. The analytical representation of in-line forces acting on a riser presented by Carberry et al.⁶ is used herein to model the external fluid force acting in the x -axis as shown in Eq. (2)

$$F_{T_x}(z,t) = \rho S C_m \dot{U}_1 - \rho S C_i \ddot{u}_x + \frac{1}{2} \rho D (U_1 - \dot{u}_x) |U_1 - \dot{u}_x| \left[C_{Dmean} + C_D \sin(2(2\pi f_L + \phi_{drag})) \right] \quad (2)$$

The density of the surrounding fluid is denoted by ρ , the cross-sectional area of the displaced fluid by S , the steady velocity of the fluid in the in-line direction acting on the surface of the structure is defined by U_1 , and D is the diameter of the riser. The mean drag coefficient is denoted by C_{Dmean} , the fluctuating drag coefficient by C_D , the inertia coefficient by C_m and the added-mass coefficient is defined by C_i . f_L is the dominant frequency defined as the most dominant frequency in the y -axis or cross-flow direction based on the fact that transverse response in flexible risers is a multi-frequency phenomenon. ϕ_{drag} is the phase of the drag with respect to the cylinder's displacement in the cross-flow direction. It is widely recognized that the dominant frequency of the drag force is 2 times the dominant frequency in the cross-flow direction ($2f_L$). Therefore, ϕ_{drag} is used to relate the phase of the drag to the displacement of the riser in the cross-flow direction and it is experimentally derived from drag traces whose correlation coefficient with a sinusoidal signal is greater than 0.6 as proposed by Carberry et al.⁶. The dominant frequency is related to the cross-flow motion and is used to calculate the transverse force as shown in Eq. (3).

$$F_{T_y}(z, t) = \frac{1}{2} \rho D U_0^2 C_L \sin(2\pi t f_L + \phi_{liff}) \quad (3)$$

U_0 is the relative in-line maximum velocity. C_L is the lift coefficient and ϕ_{liff} is the phase with respect to the cross-flow displacement. f_L mainly depends on the Keulegan-Carpenter (KC) number and the Strouhal (S_t) number. According to Blevins⁸, in-line amplitude and its corresponding KC number can be analytically and approximately related with f_L by using the expression $f_L \approx 0.2(KC f)$, where f is defined as its corresponding in-line frequency. The quasi-steady approach is a simplification of a complex phenomenon in which the motion in the cross-flow direction due to vortex shedding from a riser is represented by a sinusoidal motion. The number of variables involved in this phenomenon is considerable and there are still serious limitations in describing properly the behavior of these variables. Obasaju et al.⁴ showed that the vortex patterns around a circular cylinder in oscillating flow can be approximately divided into five regimes, namely the asymmetric ($4 \leq KC \leq 8$), the transverse ($8 \leq KC \leq 15$), the diagonal ($15 \leq KC \leq 22$), the third vortex ($22 \leq KC \leq 30$), and the quasi-steady ($KC \geq 30$). Each of these regimes is characterized by an approximate dominant frequency.

2.1 Amplitude-dependent Lift Model

Sarpkaya⁷ decomposed the instantaneous cross-flow force using a two-coefficient model into inertia and drag components in order to study its dependence on the cross-flow amplitude. It was found by Sarpkaya⁷ that the maximum negative amplitude of the drag component of the cross-flow force is achieved around $A_y/D = 0.5$ and then decreases. The oscillations become self-limiting for A_y/D larger than about unity. As noted by Sarpkaya¹, the larger the amplitude of VIV oscillations, the more nonlinear is the dependence of the lift forces on A_y/D . Based in the aforementioned facts, Blevins⁸ proposed an empirical formulation to represent the variation of the lift coefficient with respect to the amplitude of the cross-flow motion A_y . The three-term polynomial derived by Blevins⁸, presented in Eq. (4), is used in this paper to calculate the lift coefficients required for the numerical implementation of Eq. (2). Basically, the empirical formulation presented by Blevins⁸

assumes that as A_y approaches to $1D$, a breakdown of regular vortex street is produced and the value of the lift coefficient approaches to zero.

$$C_L = 0.35 + 0.6 \left(\frac{A_y}{D} \right) - 0.93 \left(\frac{A_y}{D} \right)^2 \quad (4)$$

2.2 Increased Mean Drag Coefficient Model

Sarpkaya¹ defined synchronization or lock-in as a phase transformer due to the fact that synchronization produces a rapid inertial force decrement and a rapid increment of the absolute value of the drag force. Sarpkaya¹ stated that synchronization is achieved when the reduced velocity U_r , ($U_r = U_1 / (f_{osc} D)$ and f_{osc} is the oscillating frequency of the body), reaches a value between 4 and 8. Park et al.⁹ based on numerical and experimental data concluded that it is only possible to achieve good agreement between experiments and numerical simulation if enhanced drag coefficients due to vortex induced vibrations are considered. Khalak and Williamson¹⁰ presented an empirical formulation for the increased drag coefficient, which is shown in Eq. (5).

$$\frac{C_{Dinc}}{C_{Dmean}} = 1.0 + 2.0 \left(\frac{A_y}{D} \right) \quad (5)$$

where C_{Dinc} is the increased mean drag coefficient when the oscillation frequency coincides with the shedding frequency. Khalak and Williamson¹⁰ highlighted the importance of appropriately defining the oscillation frequency and based on their experimental study found that the “classical” definition of synchronization as “frequency matching” between the oscillating frequency and the natural frequency of an oscillating body is not appropriate for the low mass-damping ($m^* \zeta$) case, where m^* is the mass ratio calculated as the mass of a body divided by the mass of the fluid displaced and ζ is defined as the ratio of ((structural damping)/(critical damping)). Khalak and Williamson¹⁰ concluded that a more appropriate definition of synchronization for the low mass-damping ($m^* \zeta$) case can be stated as the matching of the frequency of the periodic wake

vortex mode with the body oscillation frequency. This statement is adopted in the response prediction model presented in this paper.

3. Experimental Validation

In recent years, several experiments have been conducted in order to validate response prediction models for risers. Chaplin et al.³ conducted a series of experiments using a riser model in stepped current and by comparing the experimental data with 11 different numerical models found that the in-line and cross-flow displacements were under predicted by 20% to 40% and by 10% and 30%, respectively. On the other hand, risers are usually subjected to a combined loading of waves and currents. Therefore, some of the riser models have been tested under oscillatory flow or oscillating body conditions as previously explained. Duggal and Niedzwecki¹² conducted a large-scale experimental study to investigate the dynamic response of a riser model and concluded that the cross-flow response show similarities with previous research work using oscillatory flow in rigid cylinders. More recently, Jung et al.¹³ tested a highly flexible free hanging pipe in calm water and proved that in-line displacements were well predicted at the upper part of the model, but some differences were found in the lower part due to large interaction between in-line motion and vortex-induced transverse motion. Riveros et al.¹⁴ experimentally validated a response prediction model for flexible risers using a 35-meter riser model tested under lock-in considerations. Good agreement in amplitude response was observed.

In this paper, large-scale experiments are conducted to validate the proposed prediction model. A 20-meter riser model, pinned at its both ends, is sinusoidally excited at its top end using values of KC numbers in the asymmetric, transverse, diagonal and third vortex regimes (Obasaju et al.⁴). The forced oscillation experiments are carried out in the deep-sea basin of the Integrated Laboratory for Marine Environmental Protection located in the National Maritime Research Institute (NMRI). This deep-sea basin is depicted in Fig.2 and consists of a circular basin (depth: 5m, effective diameter: 14m) and a deep pit (depth: 30m, effective diameter: 6m). The underwater 3-dimensional measurement equipment is composed of 20 high-resolution digital cameras (2 units/set x 10 sets). The properties of the model are presented in Table 1. Fig.3 shows the

experimental model placed in its initial position before being excited. Its coordinate system is defined in the x -axis by the in-line motion, the y -axis corresponds to the transverse motion and the z -axis is defined in the direction of the riser's axis as illustrated in Fig.1. The model is excited in still water and steel bars are added to the riser model in order to increase its self-weight. The total weight of the riser, including the steel bars, is 68.14 N. The tension force applied at the top end of the model in the z -axis corresponds to a value of 63.5 N. A load-cell fixed to the top end of the riser is attached to the force oscillator. The variation of the tension measured by the load-cell is about 5% of the initial tension during the excitations. Thus, in this analysis, the variation of tension in Eq.(1) is assumed to be negligible. The experimental validation of the proposed response model is carried out for four different values of amplitudes and periods regarding the oscillation force at its top end as shown in Table 2. Lie and Kaasen¹⁵ presented an analytical procedure to calculate the eigenfrequencies of a long flexible riser providing good approximation if tension variation is moderate. Therefore, the n th eigenfrequency for a tensioned beam, $f_{n,t-beam}$, can be obtained as shown in Eq. (6). Using the aforementioned procedure, the analytical values of the first 4 eigenfrequencies of the riser model presented in this paper are 1.06, 2.11, 3.18 and 4.24 Hz, respectively.

$$f_{n,t-beam} = \sqrt{\frac{n^2 T_t}{4m_0 L^2} + \frac{n^4 \pi^2 EI}{4m_0 L^4}} \quad (6)$$

Table 1 Properties of the riser model

Material	Polyoxymethylene
Model length (m)	20
Outer diameter D (m)	0.0160
Inner diameter (m)	0.0108
Density (kg/m ³)	1410
Moment of inertia, I (m ⁴)	2.55E-9
Young's modulus, E (MPa)	2.937

Table 2 Harmonic excitation force

Case	Amplitude (m)	Period (sec.)	KC Number	Regime
1	0.020	2	7.9	asymmetric
2	0.027	3	10.6	transverse
3	0.040	2	15.7	diagonal
4	0.060	4	23.6	third vortex

3.1 Numerical Implementation

The Finite Element Method (FEM) is used herein to numerically solve the differential equation governing the static and dynamic response of a flexible riser presented in Eq. (1). The commercial software ABAQUS is selected to carry out this numerical implementation. The riser is modeled as an assembly of 40 cubic pipe elements. Therefore, the actual shape function of a nonlinear beam is more closely fit due to the element cubic shape functions employed in this procedure. Geometric nonlinearity is considered by using a nonlinear time-domain method during the application of the riser's self-weight. The dynamic response of the riser is then computed employing the direct-integration method. An in-house FORTRAN subroutine (developed by the authors) computes displacements, velocities and accelerations at each time step in order to generate the data needed for the numerical implementation of the amplitude-dependent lift and increased mean drag coefficient models. The in-house FORTRAN subroutine consists of three main parts. The first part collects information from the FE model without being excited in the cross-flow direction. During the first stage, it is computed the required time of the traveling wave to completely excite the riser in addition to representative values of in-line displacements and velocities. The second part of the subroutine uses the results in terms of displacements to update in-line hydrodynamic coefficients. Then, using a fixed value of C_L , cross-flow forces are subsequently applied in order to obtain a new set of updated values to be used for calculation of in-line hydrodynamic force coefficients. The subroutine then computes cross-flow displacements and velocities and performs the same updating process for C_L . Having updated values for both in-line and cross-flow hydrodynamic coefficients; the third part of the subroutine computes C_{Dinc} and carries out the final stage of the simulation. ABAQUS is used to solve the FE model; the in-house FORTRAN subroutine controls all the stages of the

simulation using external txt files to copy and read displacements and velocities at every stage of the simulation.

Carberry et al.⁶ experimentally proved that the wake states for forced oscillations are remarkably similar to the response branches of elastically mounted cylinders. Khalak and Williamson¹⁰ found an intermittent switching between the upper and lower branch amplitudes and phase angles in the cross-flow direction. On the other hand, there is a hysteretic response from the initial to the upper branch. Both of the mode transitions are related to jumps in amplitude and frequency and a 180° jump occurs only when the flow moves between the upper and the lower branches. This complex hysteretic behavior adds uncertainties to the numerical implementation of Eq. 2. The identification of the exact value at which an increment of the reduced velocity produces a jump to a new branch cannot be assessed with good accuracy considering the length of the riser model presented in this paper. Therefore, $\phi_{lift}=0^\circ$ is assumed for this numerical implementation. The value of the phase angle, ϕ_{drag} , is obtained from Carberry et al.⁶. They found that the nature of the in-line motion tends to be less sinusoidal than the cross-flow motion showing a jump of approximately 240° in the transition between the lower and initial branches. The variability of ϕ_{drag} is markedly larger than ϕ_{lift} , but when the shedding frequency matches the oscillating frequency its value tends to be zero. $C_D=0.3$ according to Carberry et al.⁶.

The KC numbers achieved by the riser model presented in this paper correspond to the asymmetric, transverse, diagonal and third vortex regimes. It is important to highlight that Lin et al.¹⁶ identified the existence of a region located around KC=10 where there is a rapid rise of C_{Dmean} and decrease of C_M . The mean drag coefficient rises approximately from 1.5 at KC=6 to 2.0 at KC=10. According to Lin et al.¹⁶, two-dimensional simulation around KC=10 fails to predict this peak due to three-dimensional flow features. On the other hand, there is a rapid decrease of C_M in the same region ($6 < KC < 10$). Obasaju et al.⁴ presented a comprehensive study of a circular cylinder in planar oscillatory flow at KC numbers ranging from about 4 to 55. It was experimentally proved that there is a range of the beta parameter ($\beta=Re/KC$) in which C_{Dmean} is not sensitive to changing β . It was also identified that the upper boundary of range lies between $\beta=964$ and 1204. The maximum

value of the beta parameter achieved by the riser model is 128. Therefore, inertia and drag coefficients experimentally computed by Obasaju et al.⁴ at $\beta=196$ are used for the numerical implementation of the proposed prediction model. The simulation results presented by Lin et al.¹⁶ are used for $KC<4$. Finally, large-amplitude vibrations due to synchronization events and a low mass-ratio value are the main characteristics of the long flexible riser model presented in this paper. Therefore, a structural damping ratio of 0.3% was included in the prediction model using as a reference the value of the structural damping ratio presented by Huera-Huarte et al.⁵. It is also important to highlight that during synchronization, the riser vibration is only limited by its structural damping. However, once the amplitude reaches about 1D, its vibration becomes self-limiting. Blevins⁸ stated that in-line VIV usually occurs with twice of the shedding frequency in the range $2.7<U_r<3.8$. The occurrence of both in-line and cross-flow synchronization events is carried out by computing the reduced velocity U_r at each time step and if its value is located in between 2.7 and 3.8, the fluctuating drag force part of Eq. (2) is included in the calculation. On the other hand, if U_r is located in between 4 and 8, the increased mean drag coefficient model is used to compute the magnitude of the drag force.

In the numerical implementation of the proposed prediction model, hydrodynamic forces are first applied using fixed values of drag and added-mass coefficients. These forces are applied during 25 cycles. Then, at the end of the first stage, in-lines amplitudes are calculated and used to update the drag coefficients based on KC values, at the same time the cross-flow forces are applied during 10 additional cycles. Synchronization events in both in-line and cross-flow are included in the third stage when drag and lift coefficients are updated. This stage lasts 45 additional cycles. The computation of the in-line and cross-flow forces is carried out by the in-house FORTRAN subroutine and then input to the FE model of the riser at each time step. The dominant frequency mainly depends on KC and S_r . Therefore, S_r is numerically calculated based on the empirical formulation proposed by Norberg¹⁷. On the other hand, although the riser model is sinusoidally excited at its top end, its dynamic response is transient due to a time-varying load. It takes approximately 4 seconds for the wave to completely excite the bottom end of the riser; then, the steady response is achieved and all sections of the model are

sinusoidally excited at different frequencies, amplitudes and phase angles. As a result, each section of the riser is excited at a particular dominant frequency in the cross-flow direction, which indeed is related to its corresponding in-line amplitude. Therefore, a phase angle must be calculated for the numerical implementation of Eq. (2) only when the steady response is achieved. Otherwise, wrong in-line amplitudes obtained during the transient response may under-estimate the phase angle and lead to out-of-phase response between the in-line and the cross-flow motions of the riser. A numerical procedure is implemented in the proposed prediction model using the top end of the model as a reference. The initial phase angle is then calculated using the time difference between the time required for each section of the model to achieve its maximum in-line displacement and the required time at the top end to achieve the same condition.

3.2 Simulation Results

The experimental validation of the proposed prediction model is conducted at 4 different regimes based on the classification provided by Obasaju et al.⁴ As shown in Table 2, the amplitudes and periods of the harmonic excitation force provide experimental validation on a wide range. In addition, the region around $KC=10$ where there exist a large variation in the values of hydrodynamic force coefficients is included in this study. The experimental data were passed through a 6th order high-pass Butterworth filter with a 0.1 Hz cutoff. The in-line phase angles were corrected in order to improve the quality of the graphical results. Variations in the phase angles were found when the experimental results were compared with simulation results. These variations may be caused in part by the initial unsteady response of the riser.

Figs.4 and 5 show the values of maximum displacements (normalized by the diameter of the riser) in both in-line and cross-flow directions for cases 1 and 2. In-line and cross-flow displacements are computed every 2 meters and correspond to x -axis and y -axis, respectively. It can be observed that the proposed model predicts in-line response relatively well in both amplitude and frequency content. It is also possible to observe some differences in the in-line direction. Especially, those regions of the riser excited at KC values in between 4 and 8. As previously explained, there is a large variation in both drag and added-mass coefficients in this region. It is also important to highlight that

inertial force affects more significantly the dynamic response of the riser at low KC values. Therefore, the different values of beta parameter used in the experimental data provided by Obasaju et al.⁴ and the riser model may cause some deviations in the response prediction. Finally, an inflection point may also have some implications in the response prediction model due to a variation of in-line amplitudes. The experimental data for case 1 show the location of an inflection point around $z=-10$ m.

Maximum cross-flow displacements show larger variation when compared with their corresponding experimental values. It is important to notice that there is a linear relationship between in-line amplitude and its corresponding cross-flow force. Fig.4 clearly shows that the theory described in this paper cannot properly explain the increment in cross-flow displacement when there is a reduction in its corresponding in-line amplitude. The simulation results follow this trend and therefore it is possible to observe a reduction in cross-flow displacement around $z=-12$ m. Figs.6 and 7 show experimental and computed values of in-line and cross-flow frequencies. The analytical values presented in Fig.6 and 7 are computed using in-line amplitudes obtained from their corresponding experimental values. Therefore, it is expected that the computed analytical values agree well with their corresponding experimental values. However, it can be seen that there are large and scattered differences and that the analytical values are closer to the simulation results in the majority of the calculations. It is possible to observe in Fig. 7 that the frequencies calculated for experimental values do not vary along the length of the riser. The main limitation in predicting such behavior is that local response from one region may dominate the total response of the riser by disrupting the excitation process in other regions (Lucor et al.¹⁸).

To provide a better interpretation of the simulation results, Fig. 8 shows the time history response of the riser during 14 seconds for case 2. It is possible to observe some variations in in-line amplitude due to nonlinear effects that cannot be accounted using numerical simulation. Cross-flow motion is irregular in both amplitude and frequency content and the approximation provided by the proposed prediction model follows the main trend of the cross-flow motion. To date, there is no model that can numerically account such irregularity in both amplitude and frequency. Figs.9 and 10 show the values of maximum displacements (normalized by the diameter of the riser) in both in-

line and cross-flow directions for cases 3 and 4. In-line displacements are well predicted. Due to the fact that in the diagonal and third vortex regimes drag forces are more dominant. On the other hand, cross-flow displacements show larger values ($A_y/D > 0.5$). Therefore, the cross-flow motion becomes more nonlinear and its prediction also becomes more challenging. Figs.11 and 12 show experimental and computed values of in-line and cross-flow frequencies. Nonlinear effects affecting response prediction are also shown in terms of frequencies. It can be seen in Fig. 12 that the riser is excited along its length in different modes and at different frequencies leading to a modal response dominated by mode interference, multimode response, mode switching and frequency dependence of the added mass. It is important to note that outside synchronization regions the force experienced by the riser will contain both the Strouhal and body oscillations (Sarpkaya¹). On the other hand, synchronization causes the matching of the vortex shedding and oscillation frequencies leading to “an increase in the spanwise correlation of the vortex shedding and a substantial amplification of the cylinder’s vibrational response” (Willdem and Graham¹¹).

Another important factor to be considered is the low mass-damping parameter of the riser model presented in this paper. According to Willdem and Graham¹¹, at low values of mass ratio, the fluid is dominant over the structure leading to a joint response dominated by the fluid and therefore their joint response frequency will be controlled by the Strouhal frequency. Actually, the accurate prediction of the cross-flow response in flexible risers is still challenging due to its highly nonlinear nature. In addition, the assumption that only one frequency dominates the cross-flow response may introduce considerable deviations in its numerical calculation. Finally, according to Morse and Williamson¹⁹ for very low-mass damping, the energy dissipated is very low, and thus the phase is close to 0° or close to 180° . It seems that a more powerful scheme using an appropriate model for the calculation of the phase angle can somehow account for this deviation. The main difficulty is that the development of such model involves challenges such as the exact location of a jump in the phase angle for a specific reduced velocity. However, based on experimental facts Morse and Williamson¹⁹ proved that even for cases of very low mass and damping the quasi-steady approximation is still valid.

3. Conclusions

A response prediction model for flexible risers was presented in this paper. Experimental data obtained from a 20-meter riser model, sinusoidally excited at its top end, were used to validate the proposed prediction model. A quasi-steady model was used to predict the cross-flow response using amplitude-dependent lift coefficients. It was also employed an increased mean drag coefficient model in order to consider drag amplification during synchronization events. The range of experimental validation provided in this paper considers the asymmetric, transverse, diagonal and third vortex regimes. Good agreement in amplitude response was found for in-line displacements. Some differences were found in the predicted response in the in-line direction for the model tested in the asymmetric and transverse regimes. This is partially caused by the large variation of the hydrodynamic force coefficients in these regions. In the transverse, diagonal and vortex regimes, the proposed model predicts relatively well in-line response. It is important to highlight that in this paper it is assumed amplitude-dependent lift coefficients. Therefore, cross-flow response is more accurately predicted when $A_y/D < 0.5$. As previously mentioned, VIV oscillations become more nonlinear when $A_y/D > 0.5$. Most of the cross-flow displacements achieved by the experimental model presented in this paper are located beyond the aforementioned limit. The fact is that no existing numerical model can really predict the dynamic response of a riser model excited in the region $A/D > 0.5$, unless very exact experimental data is previously provided for that region. It implies experiments conducted to only measure cross-flow response at that stage. Although the empirical equation used in this paper provides good approximation, it is still challenging response prediction in this region. There are so many variables included and also the degree in which are affected by large cross-flow displacements are still under intensive research even for the case of an oscillating or fixed cylinder. This paper provides simulation results of a long riser model excited under critical conditions and also provides a tool that can be used to numerically approximate its response.

The response prediction of an oscillating flexible riser involves several challenges due to the nonlinear and self-regulated nature of the VIV process. It has been sufficiently proved that synchronization events cause an increase of cross-flow displacements leading to a sudden increase in the drag force and therefore affect the whole in-line response of

the riser. The numerical results show that proposed prediction model accounts for such increments and therefore provides a good interface between cross-flow motion and its effect on in-line motion. Furthermore, the dynamic response of a flexible riser having a value of mass ratio lower than 3.3 is more complex due to the existence of 3 modes of response in contrast with the 2 modes of response found in risers having values of mass ratio larger than 10. Considering the nonlinear and self-regulated nature of the VIV process, especially during synchronization events that leads to large displacements and sudden changes in the phase angle of the lift force, this paper presents a practical methodology for response prediction of oscillation flexible risers.

References

1. Sarpkaya T (2004) A critical review of the intrinsic nature of vortex-induced vibrations. *Journal of Fluids and Structures* 19:389-447.
2. Al Jamal H and Dalton C (2005) The contrast in phase angles between forced and self-excited oscillations of a circular cylinder. *Journal of Fluids and Structures* 20:467-482.
3. Chaplin JR, Bearman PW, Cheng Y, Fontaine E, Graham JMR, Herfjord M, Isherwood M, Lambrakos K, Larsen CM, Meneghini JR, Moe G., Triantafyllou MS, and Willden RHJ (2005) Blind predictions of laboratory measurements of vortex-induced vibrations of a tension riser, *Journal of Fluids and Structures*. 21:25-40.
4. Obasaju ED, Bearman PW, and Graham JMR (1988) A study of forces, circulation and vortex patterns around a circular cylinder in oscillating flow. *Journal of Fluid Mechanics* 196:467-494.
5. Huera-Huarte FJ, Bearman PW, and Chaplin JR (2006) On the force distribution along the axis of a flexible circular cylinder undergoing multi-mode vortex-induced vibrations. *Journal of Fluids and Structures* 22:897-903.
6. Carberry J, Sheridan J, and Rockwell D (2005) Controlled oscillations of cylinders: forces and wake modes. *Journal of Fluid Mechanics* 538:31-69.
7. Sarpkaya T (1995) Hydrodynamic damping, flow-induced oscillations, and biharmonic response. *ASME Journal of Offshore Mechanics and Arctic Engineering* 117:232-238.
8. Blevins RD (1990) *Flow-induced Vibration*, Second Edition, Krieger Publishing Co., New York, USA.

9. Park HI, Jung DH and Koterayama W (2003) A numerical and experimental study on dynamics of a towed low tension cable. *Applied Ocean Research* 25:289-299.
10. Khalak A, and Williamson CHK (1999) Motions, forces and mode transitions in vortex-induced vibrations at low mass-damping. *Journal of Fluids and Structures* 13:813-851.
11. Willden RHJ and Graham JMR (2006) Three-distinct response regimes for the transverse vortex-induced vibrations of circular cylinders at low Reynolds numbers. *Journal of Fluids and Structures* 22:885-895.
12. Duggal AS and Niedzwecki JM (1995) Dynamic response of a single flexible cylinder in waves, *ASME Journal of Offshore Mechanics and Arctic Engineering*. 117:99-104.
13. Jung DH, Park HI, Koterayama W and Kim HJ (2005) Vibration of highly flexible free hanging pipe in calm water. *Ocean Engineering* 32:1726-1739.
14. Riveros CA, Utsunomiya T, Maeda K and Itoh K (2009) Dynamic response of oscillating flexible risers under lock-in events. *International Journal of Offshore and Polar Engineering*, 19(1):23-30.
15. Lie H and Kaasen KE (2006) Modal analysis of measurements from a large-scale VIV model test of a riser in linearly sheared flow. *Journal of Fluids and Structures* 22:557-575.
16. Lin XW, Bearman PW, and Graham JMR (1996) A numerical study of oscillatory flow about a circular cylinder for low values of beta parameter. *Journal of Fluids and Structures* 10:501-526.
17. Norberg C (2003) Fluctuating lift on a circular cylinder: review and new measurements. *Journal of Fluids and Structures* 17:57-96.
18. Lucor C, Mukundan H, and Triantafyllou MS (2006) Riser modal identification in CFD and full-scale experiments. *Journal of Fluids and Structures* 22:905-917.
19. Morse TL and Williamson CHK (2006) Employed controlled vibrations to predict fluid forces on a cylinder undergoing vortex-induced vibration. *Journal of Fluids and Structures* 22:877-884.

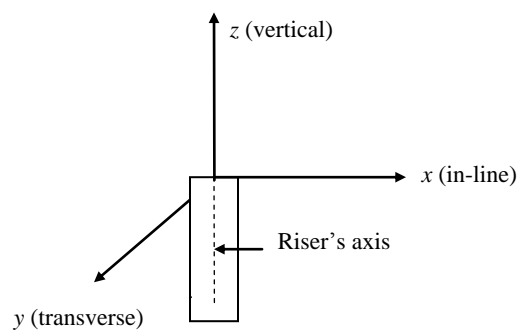


Figure 1: Riser Motion and Coordinate System

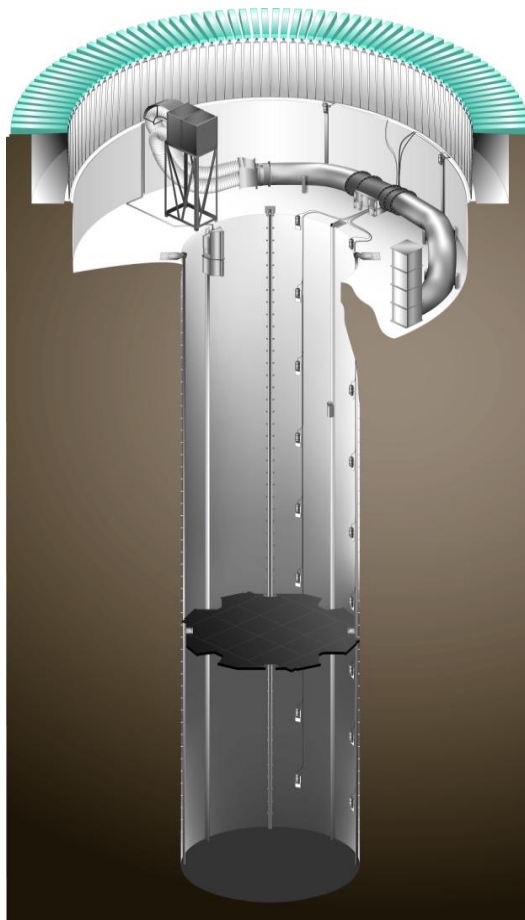


Figure 2: Deep-sea Basin (NMRI)

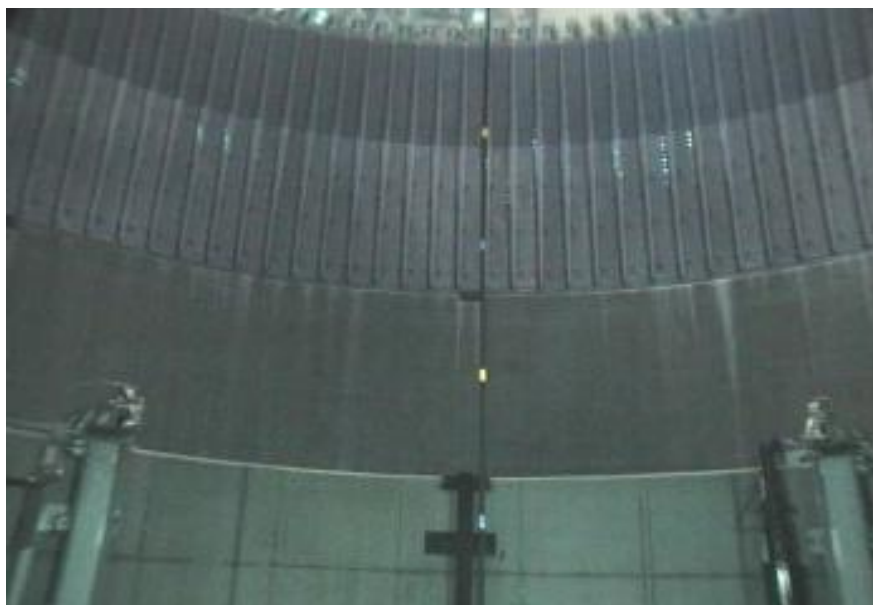


Figure 3: 20-meter Experimental Riser Model (NMRI)

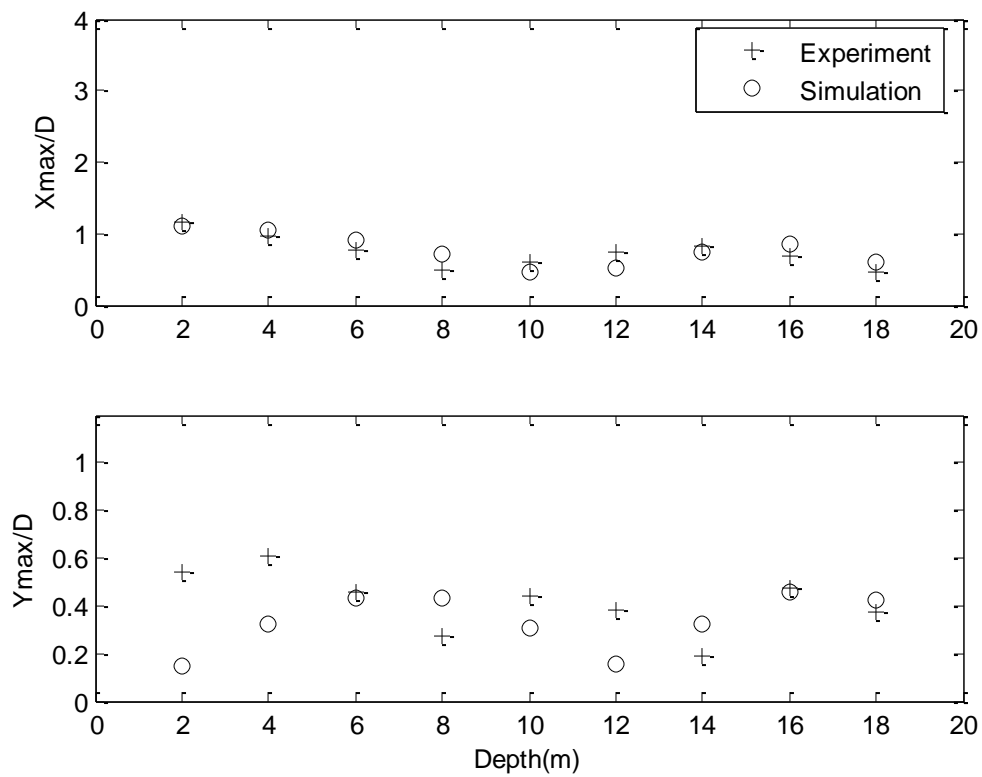


Figure 4: Maximum In-line Displacements (top row) and Cross-flow Displacements (bottom row) (Case 1)

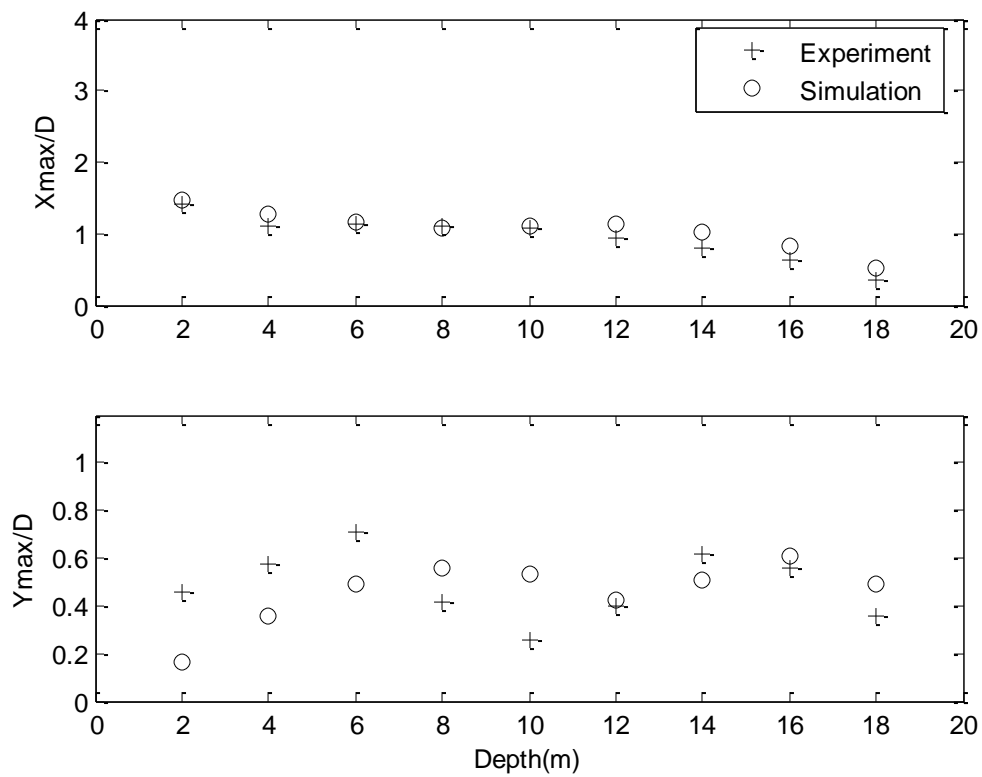
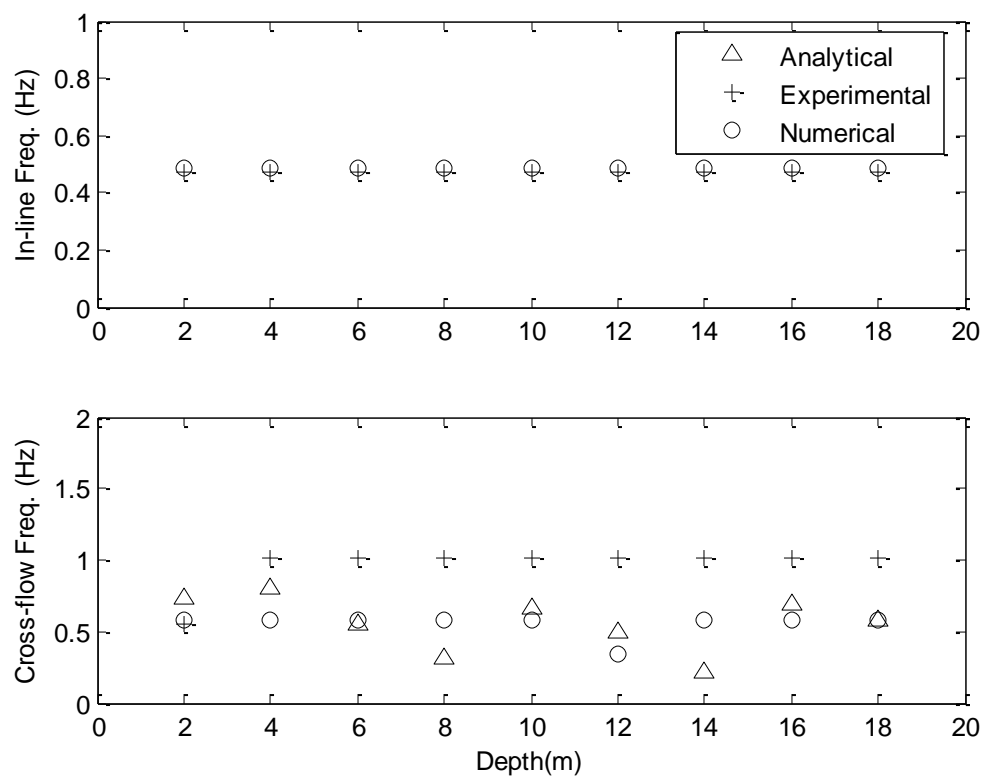
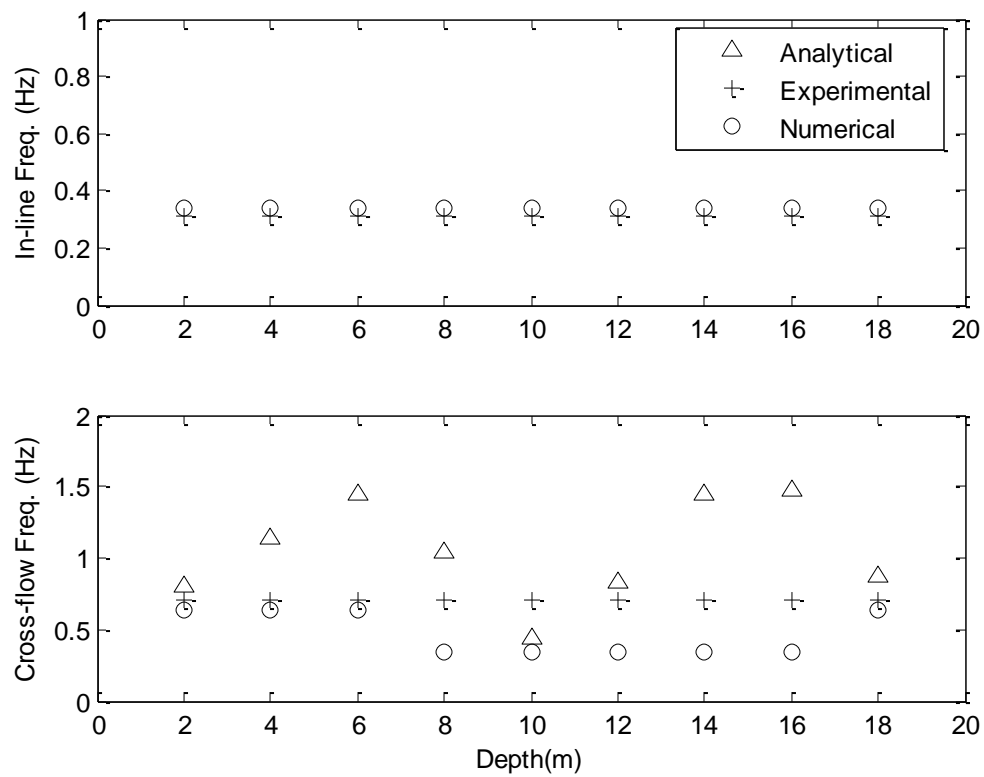


Figure 5: Maximum In-line Displacements (top row) and Cross-flow Displacements (bottom row) (Case 2)



**Figure 6: In-line Frequencies (top row) and
Cross-flow Frequencies (bottom row)
(Case 1)**



**Figure 7: In-line Frequencies (top row) and
Cross-flow Frequencies (bottom row)
(Case 2)**

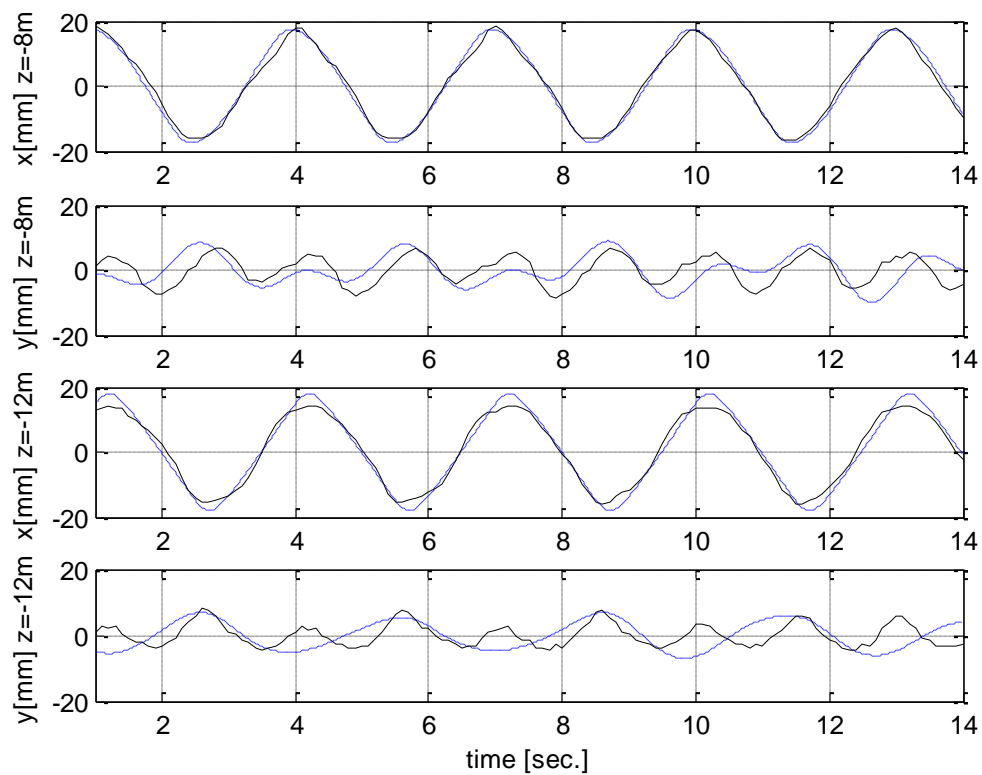


Figure 8: Time History Response at $z = -8\text{m}$ and $z = -12\text{m}$ (Case 2)
 ---- Simulation — Experiment

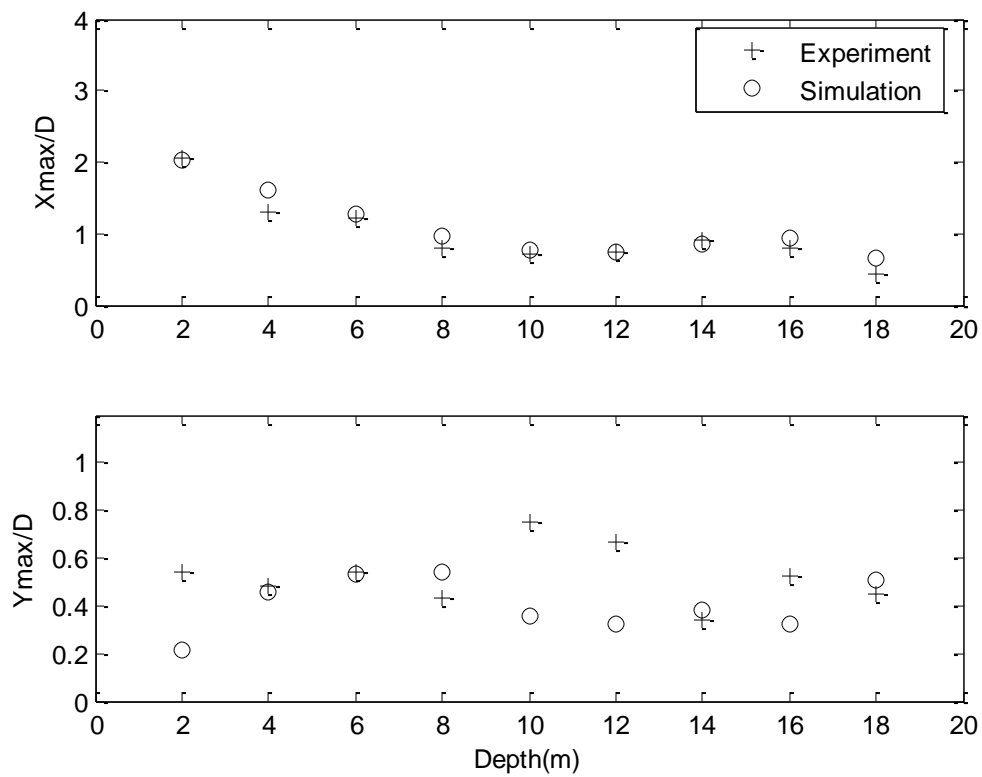


Figure 9: Maximum In-line Displacements (top row) and Cross-flow Displacements (bottom row) (Case 3)

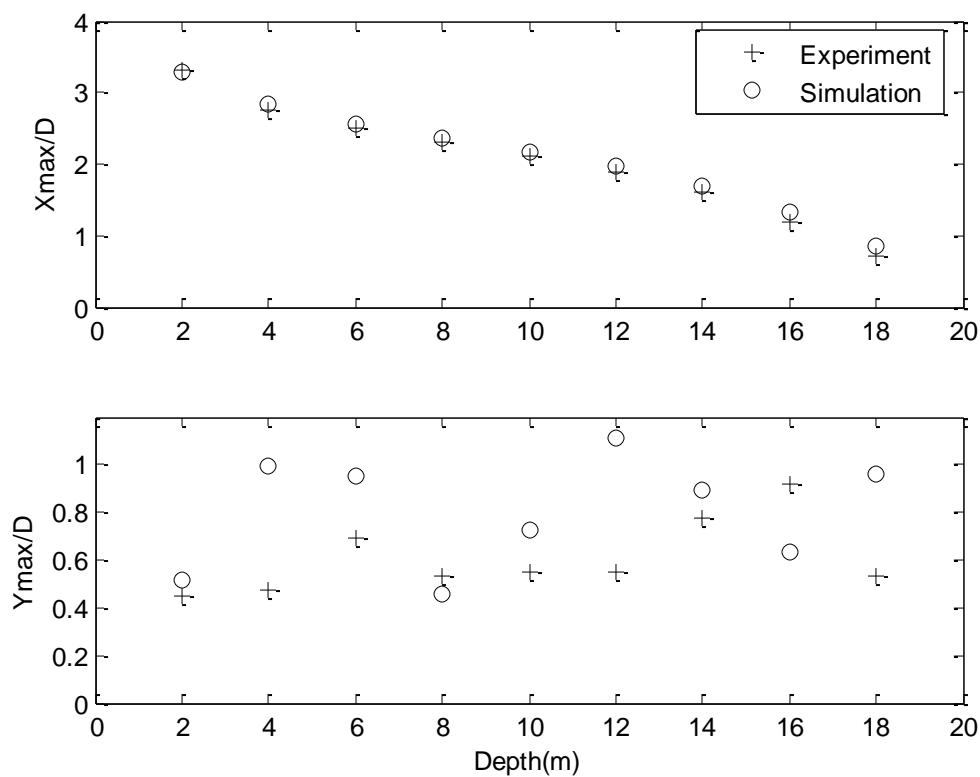
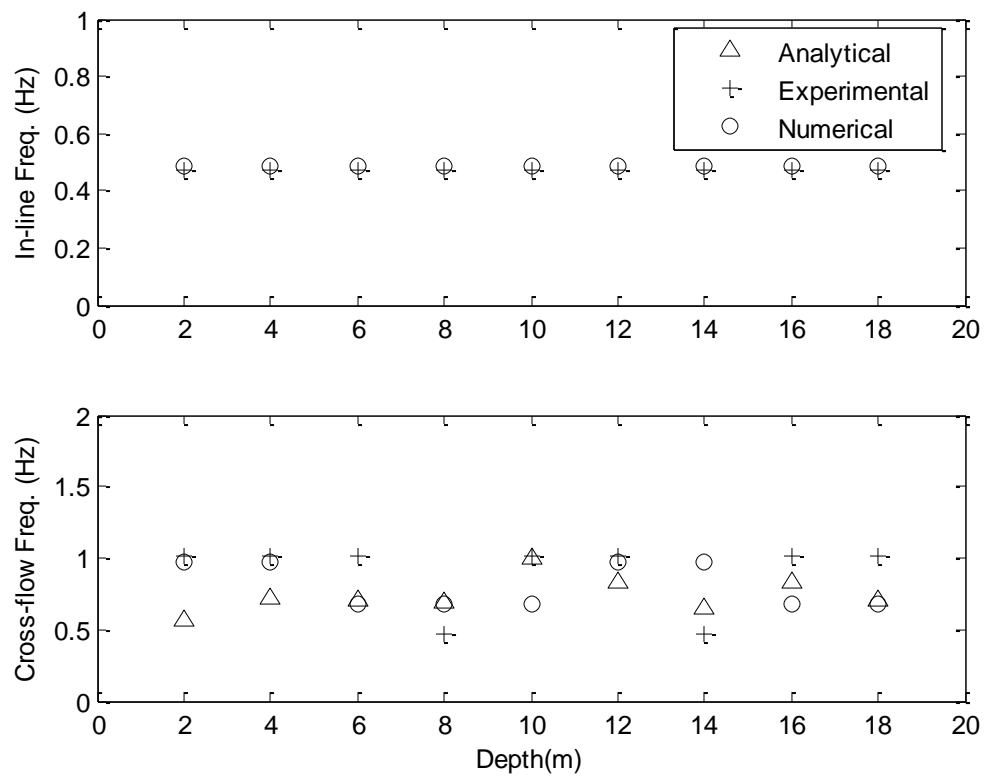
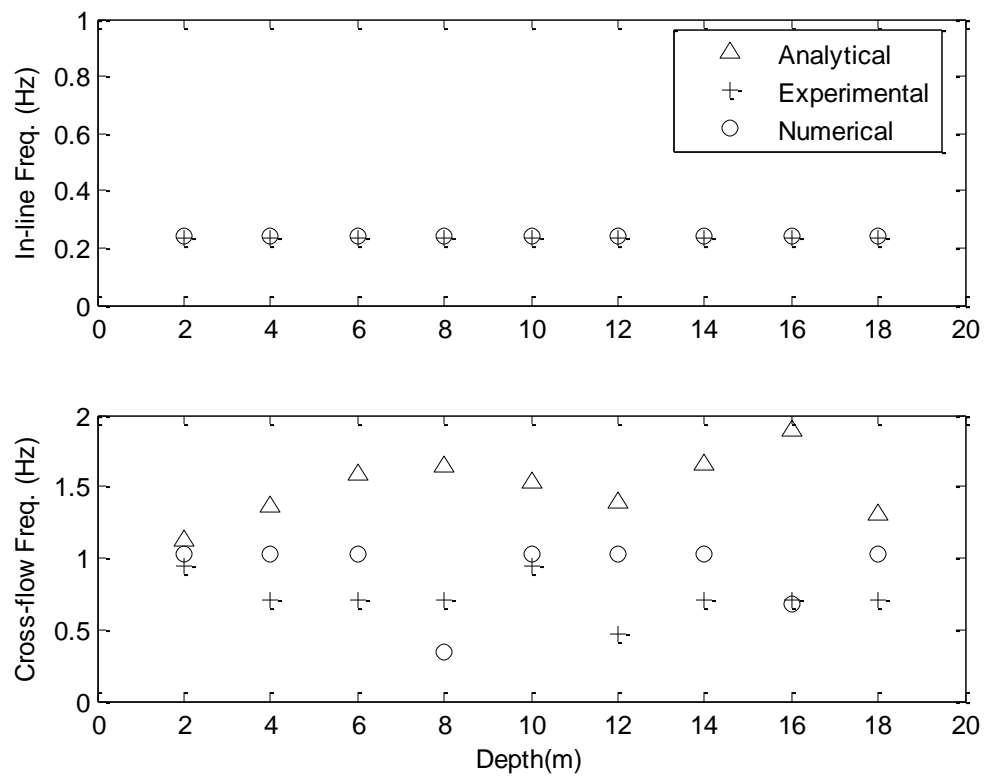


Figure 10: Maximum In-line Displacements (top row) and Cross-flow Displacements (bottom row) (Case 4)



**Figure 11: In-line Frequencies (top row) and
Cross-flow Frequencies (bottom row)
(Case 3)**



**Figure 12: In-line Frequencies (top row) and
Cross-flow Frequencies (bottom row)
(Case 4)**